Preparation and determination the optimizing effect of structure Nano-lipid loaded Honey and Platelets Growth Factor on skin wound healing in rabbit

Noor Thabit Nouman[*] and Mohanad A. Al-Bayati[*]

[*]Department. of Physiology and Pharmacology, College of Veterinary Medicine, Baghdad University.

*Corresponding author: aumnmumu@covm.uobaghdad.edu.iq

Abstract: Wound healing is the replacement of damaged tissue via highly coordinated cellular events. The patient's condition, as well as the various types of wounds, further complicate the already complex healing process. Traditional wound dressing materials appear insufficient for facilitating and supporting this mechanism. Nanotechnology has the potential to provide the physicochemical properties and specific biological responses required to aid in the healing process. The Nano lipid is used for the delivery system to improve drug delivery and concentration in the site of action by reducing dosage form adverse reaction on skin healing and improve stability and loading capacity and prevent drug/active molecule expulsion during storage. Patients and Procedures: Prepare and standardize the structure Nano lipid by the solvent diffusion method, Seventy rabbits were divided into six groups a daily dressed treatment, the full excisional wounds were treated with three different formulas: conventional $_{Honey\&PDGF}$, Structural Nano Lipid (SNL- blank), and $SNL_{Honey\&PDGF}$ gel. The linear wound healing rate $t_{1/2}$, closure velocity, and effective concentrations (ECs_{20} and $_{50}$) of SNL in honey and PDGF were all measured. Results: The electron micrograph denoted the different size for honey 73.55± 1.04 nm, PDGF 51.92± 1.13 nm, SNL_{Honey} 30.76 ±1.27 nm, SNL_{PDGF} 142.50± 0.95 nm, and $SNL_{Honey\text{-}PDGF}$ 94.22± 0.77 nm respectively. As well as, the entrapment and loading efficiency was found the actual amount efficiency values, and the loading percent of SNL_{PDGF} was 93.67 and 89.11% and SNL_{Honey} was 91.19, and 87.99% respectively. While the absorbance curve showed distinctive main wavelength for $SNL_{Honey\&\ PDGF}$ were 990.0, 230.5, and 196.0 nm also SNL_{Honey} 992.0 and 228.0, SNL_{PDGF} 989.5 and 225.0 nm compared to conventional honey and PDGF, which showed at 271.5 and 256.0 nm respectively, the XRD analysis $SNL_{Honey\text{-}PDGF}$ has sharp peaks and provided a particle size between 20 and 30 nm also SNL_{Honey} 20–40nm, but SNL_{PDGF}, honey, and PDGF are wider with lower intensities, negative Zeta potential values, however, the values to be considered stable in $SNL_{Honey\&PDGF,}$ PDGF, and honey -18.5 mV, -14.0 mV, and -20.1 mV compared to SNL_{Honey} and SNL_{PDGF} -54.2 Mv and -61.8 mV and that demined the Nano-size lesser than that aggregated form, as well as, Fourier infrared spectroscopy showed the diagnostic functional peaks in both conventional and Nano form and mimic the chemical structure was not altered and preserved the chemical behavior properties. The wound healing results revealed that Nano lipid loaded Honey&PDGF gel reduced wounds and healed faster than conventional $_{Honey\&PDGF}$; higher closure rate, closure velocity, and low closure $t_{1/2}$. The values of the $EC_{S50\ \&\ 20}$ in SNL $_{Honey\ and\ PDGF}$ according to potency (EC_{50} SNL_{Honey} 0.119, EC_{50} SNL_{PDGF} 0.353, EC_{20} SNL_{Honey} 0.129, and EC_{20} SNL_{PDGF} 0.083%) wound closure time on the skin. As well as the tissue phenomics stereology appearance the scores of inflammatory decreased score values, decreased scab and vascularization score, increased the score of collagen fiber and extracellular matrix deposition of fibroblast, as well as, the epithelialization represented with increased time of wound healing increased epithelium significantly in $SNL_{Honey\text{-}PDGF}$ compared with other treated and control groups. Conclusion: The reformulated conventional Honey& PDGF attained Nanoparticle

status by carrying it in the structure Nano lipid that $SNL_{Honey\& PDGF}$ has different advantages in delivery systems for topical application and accelerated wound healing.

Keywords: Structural Nano Lipid, honey, growth factor, wound healing

Department of Physiology, Biochemistry, and Pharmacology, College of Veterinary Medicine, University of Baghdad, Iraq

[1]Department of Physiology, Biochemistry, and Pharmacology, College of Veterinary Medicine, University of Baghdad, Iraq

1. Introduction:

Bees and other insects collect honey, a yellowish-brown, sweet, and viscous sugar solution, from the nectar of flowers (Ramli *et al*., 2018). Honey's antimicrobial, anti-inflammatory, antioxidant, immunostimulant, and debridement properties make it a natural medicine that promotes and accelerates the healing of wounds and a variety of other skin conditions. Honey also acts as a stimulant for skin regeneration and treats different types of wounds and dermatic diseases (Burlando *et al*., 2013). Growth factors are soluble proteins produced by several cell types, such as macrophages and fibroblasts, that control angiogenesis and local immune responses for wound healing (Duncan *et al*., 2018). Growth factors with significant applications in bone tissue engineering, cartilage tissue engineering, skin tissue engineering, and wound healing include platelet derivative growth factor (PDGF) (Evans *et al*., 2019).

Several attempts have been made to work on healing in various types of skin tissue for increased healing and decreased environment and internal worse interaction. Techniques and protocols maneuvers were used with known flaws that aided partially in wound healing and closure with minor or major outcomes in healing final shape and time requirement (Silva *et al*., 2018).

This research focuses on the pharmaceutics care agents on skin wounds that were subjected to various maneuvers and determined optimized remedies; first, the new scientific approaches excreted Nanopharmaceutics; a special Nano lipid delivery system to increase stability, control, and release of drug as well as drug targeting sites, reduce bolus dosage, improve pharmacokinetic bioavailability, biodegradability, The incorporation of both hydrophilic and lipophilic drugs, as well as the protection of labile drugs against chemical degradation, reduced toxicity (Campos *et al*., 2020). The objective of the study is to curable wounds with minimized impact adverse effect by determining structure Nano lipid carrying growth factor and honey under basic concept contribution of the wound healing process.

2. Experimental design

Seventy rabbits were grouped into six major groups as follows: the first group was five animals as a control group, the second group was five animals as SNL- blank, the third group was five animals as conventional PDGF treated group (2.5 ng/ml), the fourth group was five animals as conventional Honey treated group (100%). The fourth and fifth treated groups were divided into five subgroups according to the dose of concentrations infiltrated in the skin (0.5, 1, 1.5, 2, and 2.5 %) and (20, 40, 60, 80, and 100%) in SNL_{PDGF} and SNL_{Honey} respectively.

2.1. Preparation of $SNL_{Honey\& PDGF}$

Zhang et al. (2018); Buthina and Mohanad, (2023) used the solvent diffusion method to prepare and standardize the lipid status; the formulation consisted of the lipid status formed

by Stearic acid dissolved by glycerine monostearate and dispersing 800 rpm with Castor oil 2 ml to form lipid dispersion by vortex 1500 rpm for 30 minutes. The forming lipid phase was then dissolved in phosphatic acid and loaded with honey or PDGF to achieve concentrations in 1ml of dimethylformamide before dispersion at 800 rpm for 30 minutes. Following that, add the dissolving form to the lipid form and disperse for two hours at 800 rpm (Cohen *et al.*, 2012).

2.2. Mixed the gel with $SNL_{Honey\ or\ PDGF}$

The gel was formed by dissolving 0.125g of carbopol and stirring in 3ml of distilled water to form the gel phase with an equilibrated acidic feature of gel via added 1ml of NaOH 0.1N with mixed well until the suspension became thick and clear, the gel was heated for 15 minutes to freed air bubbles (Sivakumaran *et al.*, 2011), and the SNL honey or PDGF in 1 ml was mixed with gel at 0.3g v/w.

2.3. The Standardization of $SNL_{Honey\ \&\ PDGF}$

The SNL formation and functional structure of a loaded structural Nano lipid Honey and PDGF were studied and standardized using parametric maneuvers (Nawal *et al.*, 2020; Mathur *et al.*, 2014).

Light micrograph, Electron micrograph

Based on the programmed image and the metric scale, scan electron microscopy and transmission electron microscopy were used to assess the structure of Nano-lipid Honey and PDGF. The average size percentage was determined using data from Yokoyama et al (Yokoyama *et al*., 2007).

X-ray diffraction (XRD)

Using a Cu Ka radiation wavelength of 1.54060 A°, the X-ray diffraction examination of crystallization status was carried out using an X-ray diffractometer (2 to 40 C°) to evaluate the structural Nano-lipid Honey & PDGF and traditional Honey & PDGF final structural form uniformly (Zine *et al*., 2017).

Fourier Transformed Infrared Spectroscopy (FTIR)

Used to evaluate the structure Nano-lipid Honey & PDGF physical and chemical interaction, which was evaluated by spectrophotometer at a wavelength between 400 and 400 cm1 (Wang *et al*., 2014).

Zeta potential

The stability of a dispersion of Nanoparticles was tested using the zeta potential of structure Nano-lipid Honey & PDGF (Wang *et al*., 2014). Zeta size analysis was used to determine the lipid particulate dispersions' average particle size, polydispersity index, and zeta potential (DTS Ver.5.10, Malvern Instruments).

Entrapment loading and Efficiency

Using the ultrafiltration centrifugation method, the free content in the solution containing SNL was determined to estimate the entrapment efficiency (EE%) and drug load (DL). (Wang *et al*., 2016; Ali and Mohanad, 2020).

EE% = Total amount-free amount (supernatant)/Total amount× 100

DL% = Total amount of content- Amount of free content/ Total amount of lipid × 100

2.4. Induction of excisional wound of skin rabbit

Accordance with the ethical fact, the rabbit was put to sleep by having 2% of each group's lidocaine local anesthetic injected subcutaneously (Balbino *et al*., 2005).

2.5. The surgical maneuvers created wounds

The hair on the dorsal midline of each rabbit was clipped and shaved without abrading the skin,

and the area of the wound was disinfected with 70% alcohol, and the animals were placed in a suitable restraining position and oriented so that their backs could be conveniently reachable, and the circular line pattern was used to mark on bi-side back and a full-thickness of skin, fascia with muscle deep wound was made by excising the skin at 0.8 cm as a circular line, induced surgically at a depth of 0.5 mm, this procedure completely removed whole skin layers and created symmetrical excisional wounds before removing part of the muscular layer beneath the skin layers (Roaa and Mohanad, 2022; Camila *et al.,* 2015).

2.6. Wound treatment and dressing

The SNL_{Honey} gel, SNL_{PDGF} gel, and conventional $_{Honey\ and\ PDGF}$ were applied and dressed topically at the excisional wound, with the control remaining untreated. To prevent contamination, the wound was plastered and draped (Canesso *et al.,* 2014).

2.7. Wound closure monitoring post-excisional surgery

The wound area of the monitored rabbit's post-excisional surgery was evaluated and assessed every day until the complete wound closure area, A caliper was used to measure the wound area's kinetic drive during closure. According to Vidal et al. (2015), the dimensional diameters of the excisional wound area were measured on days 5, 10, 20, and 30 as follows:

$$wound\ area = \frac{diameter\ A}{2} \times \frac{diameter\ B}{2} \times \pi$$

Furthermore, Gopinath *et al.* (2004) used the following equation to calculate the percentage of kinetic wound closure:

$$wound\ closure = \frac{actual\ wound\ area\ (cm)}{Initial\ area\ of\ wound} \times 100$$

2.8. Timeline analysis of wound healing

The morphology of new tissue formation was studied and achieved at various stages of committed healing on the formed cicatricial tissue. Five slices were evaluated to include the healing wound borders (the area of the wound boundary between the edge of intact connective tissue and the one of new tissue formation) and the wound center or forming scar (Roaa and Mohanad, 2022). Cassini et al. (Cassini *et al.,* 2015) examined five wounds and five slices. The closure indices were calculated using three parameters:

1. **Closure rate**: the wound closure area per unit time during the total growing phase, as calculated by the following equation:

$$Closure\ rate = \frac{1-\frac{Intial\ wound\ area - final\ wound\ area}{intial\ wound\ area}}{Time\ (days)}$$

2. **Closure velocity**: the total time required for wound closure as calculated by the following equation (Gilman, 2004)*:*

$$Closure\ velocity = \frac{\Delta A_{\ i-f(primeter)}}{\Delta t}$$

$* \ \Delta A_{\ i-f}$ the change between the area of the excisional wound and the final closure area.

3. **T½ of wound healing**: the half-life of closure area time in treated groups, as calculated by the equation below:

$$t½\ closure = \frac{q}{Dc} : \text{where} \quad Dc = \frac{\Delta r}{\Delta t}$$

*q is the intercept, Dc continuous linear healing rate, ΔA= change alter in apparent wound area between two consecutive times of measurement, Δt= time between two certain consecutive measurements

2.9. Histological assessment of wound healing

Histological investigation of skin wound healing was conducted, and skin samples were fixed in

10% formalin solution for 24 hours before being embedded in paraffin for microscopic evaluation. Masson's trichrome staining was done after tissue sections of 4-5 m thickness were cut (Vidal *et al*., 2015; , Muhannad, 2005). The core of each existing structure was documented over time for each wound's histological qualitative structural score in stained tissues (Castro *et al* 2015; Castro *et al*., 2014).

The following grades were used to assess the inflammatory score: Grad zero included the absence of inflammatory cells and symptoms, grad two the presence of few inflammatory cells and constrained symptoms, grad three the presence of many inflammatory cells and distinctive symptoms, and grad four the presence of exaggerated inflammatory cellularity and significant symptoms (De Moura *et al.*, 2019; Fatima and Al-Bayati, 2021).

SNL-blank SNL_{Honey} SNL_{PDGF}

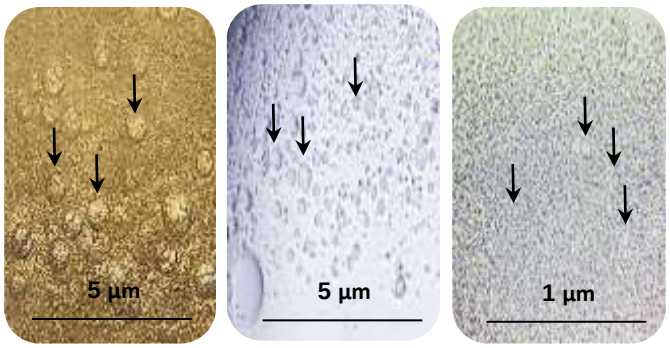

Figure 1. The photomicrograph of $SNL_{Honey,\ PDGF,}$ and blank

3. Ethics

The ACUC guideline "Laboratory Animal Care and Use handling and management of rabbits, and ethical craft pharmaceutical dosing and curative operations according to Al-Bayati and Khamas, (2015) was the basis for the ethics that were adopted.

4. Statistical analysis

The data results in analyses were done via Windows Microsoft Excels program for F test (ANOVA) one way and two ways, the significance degree level was measured as $p \leq 0.05$, and statistical comparison was achieved with less significant differences LSD (Tome, 2009).

5. Results

5.1. The Standardization of $SNL_{Honey\ \&\ PDGF}$

Table 1. The size and entrapment and loading efficiency of PDGF and Honey

Groups	The size electron micrograph		Entrapment efficiency	Loading efficiency
	mean	range		
SNL_{Honey}	30.76±1.27 e	18.46-43.07	91.19 ± 7.03 b	87.99 ± 4.62 b
SNL_{PDGF}	142.50±0.95 a	90.4-195.2	93.67 ± 9.15 a	89.11 ± 10.70 a
$SNL_{Honey-PDGF}$	94.22±0.77 b	53.84-134.61	-------	-------
PDGF	51.92±1.13 d	34.61-69.23	-------	-------
Honey	73.55±1.04 c	34.61-138.46	-------	-------

A. **B.**

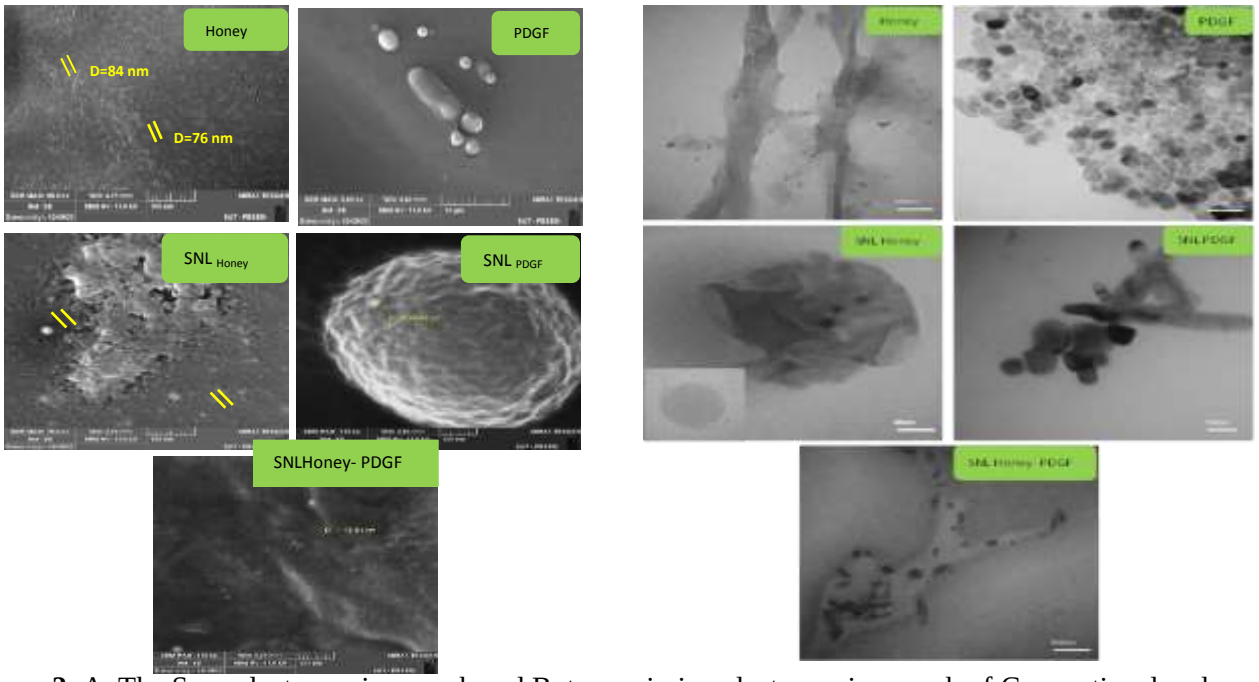

Figure 2. A. The Scan electron micrograph and B. transmission electron micrograph of Conventional and SNL of honey and PDGF and their combination

A. B.

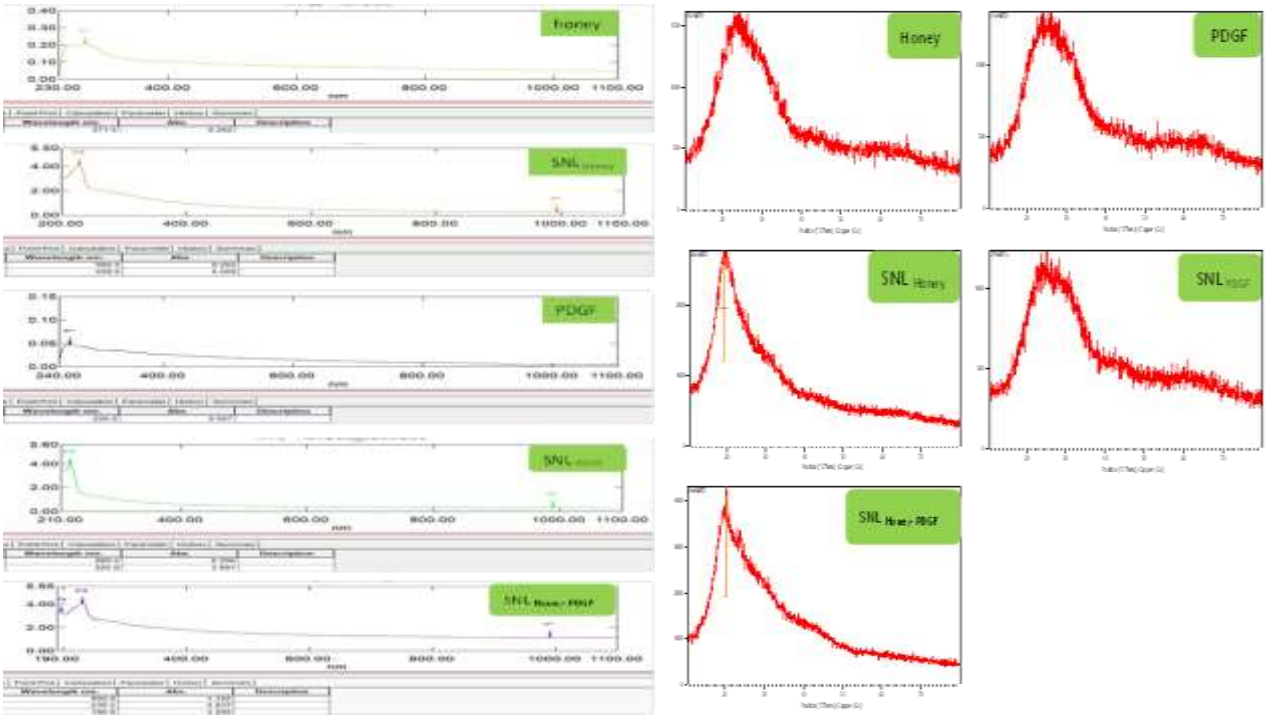

C. **D.**

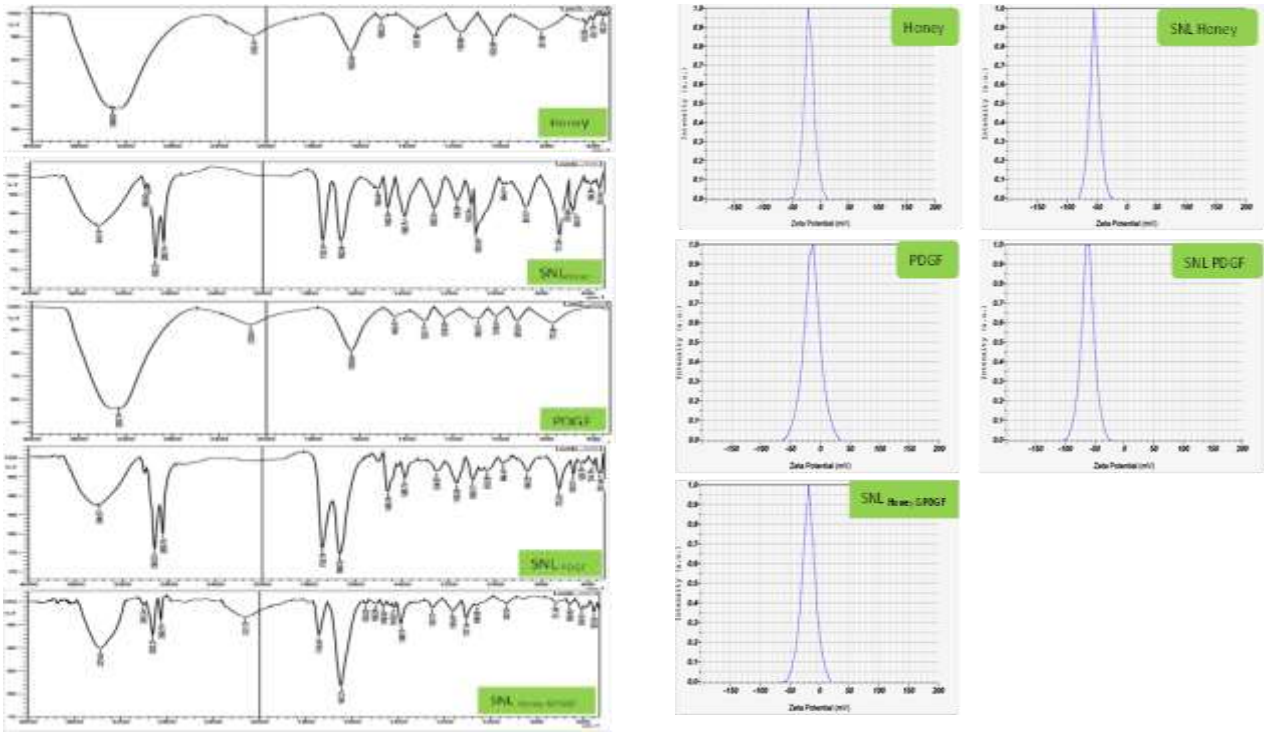

Figure 3. A. The absorbance curve, **B.** Powder X-ray Diffraction, **C.** The Fourier transformed infrared, **D.** Zeta potential of Conventional and SNL of honey and PDGF and their combination.

5.2. The closure behavior and kinetic curve of wound healing dressed formulas of SNL and conventional; honey, PDGF

The timelines of wound closure dressed the wound with honey and PDGF formula; SNL and conventional forms exhibited the behavior closure in two consecutive; growing and remodeling periods. The depiction of the wound dress showed grossly the diameter of the wound narrowed in the concentration of dress at 20% in SNL_{Honey} and 1% SNL_{PDGF} than others with prior remodeling than other treated wounds. The kinetic of wound closure was significantly ($p \leq 0.05$) as based on time versus closure area is ordered faster as in the following respectively.

Days	27.32	28.41	31.21	32.84	33.54	34.22	36.15	37.11
Groups	SNL $_{Honey}$ G 20%	< SNL $_{Honey}$ G 40%	< Con H 100%	< SNL $_{Honey}$ G 60%	< SNL $_{Honey}$ G 80%	< SNL $_{Honey}$ G 100%	< SNL-$_{blank}$	control

Days	27.22	29.73	30.82	35.51	35.31	35.14	36.15	37.16

Group $\text{SNL}_{\text{PDGF}}\text{G}$ 1% < $\text{SNL}_{\text{PDGF}}\text{G}$ 0.5% < $\text{SNL}_{\text{PDGF}}\text{G}$ 1.5% < $\text{SNL}_{\text{PDGF}}\text{G}$ 2% < $\text{SNL}_{\text{PDGF}}\text{G}$ 2.5% < Con PDGF 2.5% < $\text{SNL}_{\text{blank}}$ control

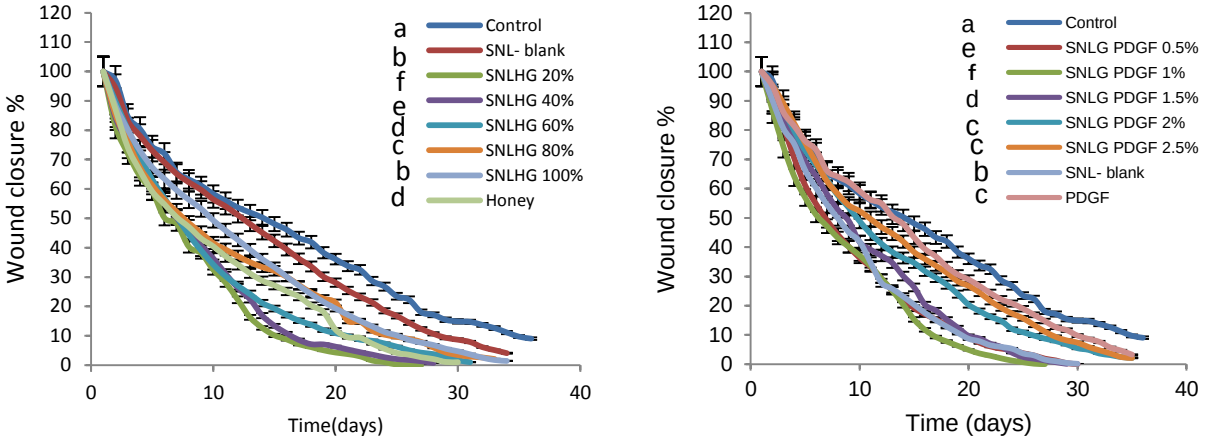

Figure 4. Wound healing curve behavior in series concentrations of structural Nano lipid Honey, PDGF per timeline in the growing and remodeling phase

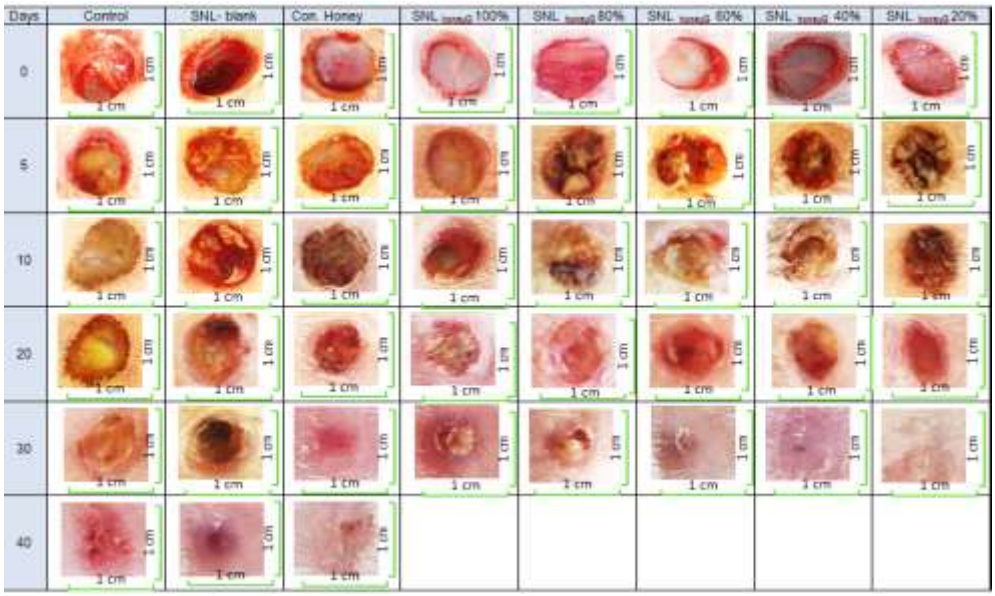

Figure 5. The depiction of wound growth kinetic development in time track local treated by control, SNL-blank, conventional $_{\text{Honey}}$, and $\text{SNL}_{\text{Honey}}$ Gel at different concentrations.

Figure 6. The depiction of wound growth kinetic development in time track local treated by the concentration of SNL_{PDGF} was observed according to the ordered days

5.3. The wound kinetic curve dressed honey and PDGF formulas Structural Nano-lipid and conventions

The timeline of wound closure in the growth phase and wound healing in remodeling was determined according to the time kinetic closure curve. The growth phase was a collapse in $SNL_{Honey}G$ at 20% between 0-17 days and remodeling 17-27 days significantly ($p \leq 0.05$) as compared with other timelines dressed the wound. The growth phase duration decreased in the group of $SNL_{PDGF}G$; by 1%, between 0-18 days and remodeling by 18-27 days significantly ($p \leq 0.05$) as compared with other timelines dressed the wound of groups control and dressed groups 0.5%, 1.5%, 2%, and 2.5% showed reversed effect and delay healing were displayed in figure (7 and 8).

5.4. The dose-response curve of wound healing of structural Nano-lipid, conventional honey-PDGF

The wound healing indices were expressed as a Log dose-response curve and determined the potencies. The data is presented in figure (9). The curve context of linear rate and velocity of wound healing showed progressive steady increased values with concentrations increase among control 0 to 20% of dressed wound groups then tend to the plateau at dressed wound concentration 40% then upset post dressed wound concentration 60% to 100%. While the curve of closure $t_{1/2}$ of wound healing showed a progressive steady decrease value augmented with an increase between groups dressed wounds in control 0 to 20% then tend to plateau at 40% then followed deviated to upset post groups dressed wound concentrations 60% to 100% SNL formula concentrations displayed retardation represented prolong of healing closure $t_{1/2}$.

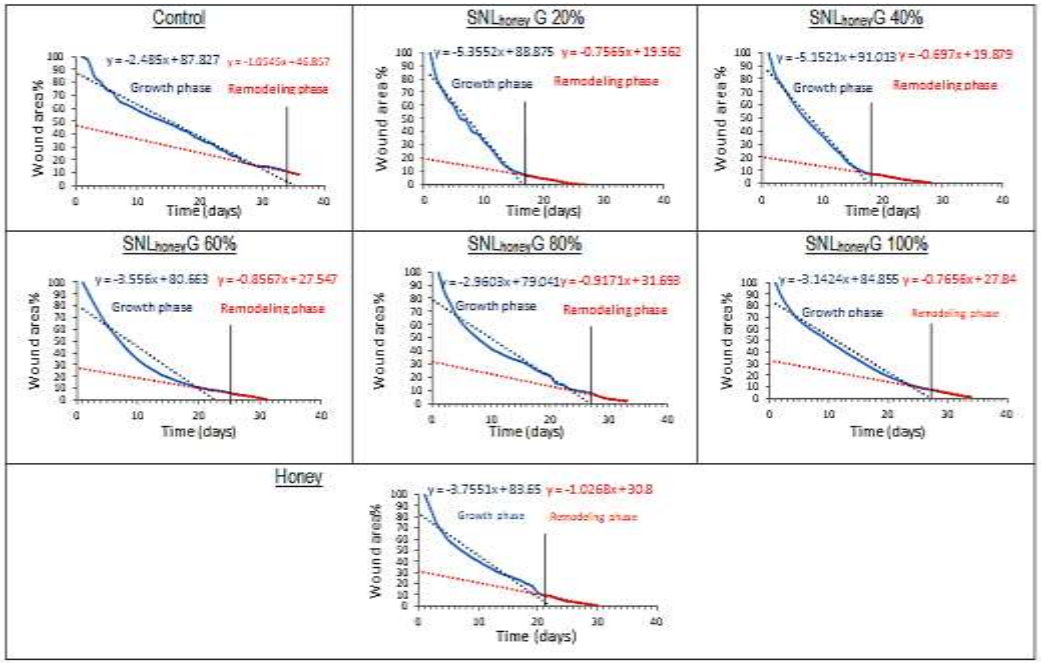

Figure 7. The comparison between wound healing kinetic curves of individuals concentration in two phases; growing and remodeling phases, in conventional and structural Nano-lipid honey-dressed formulas.

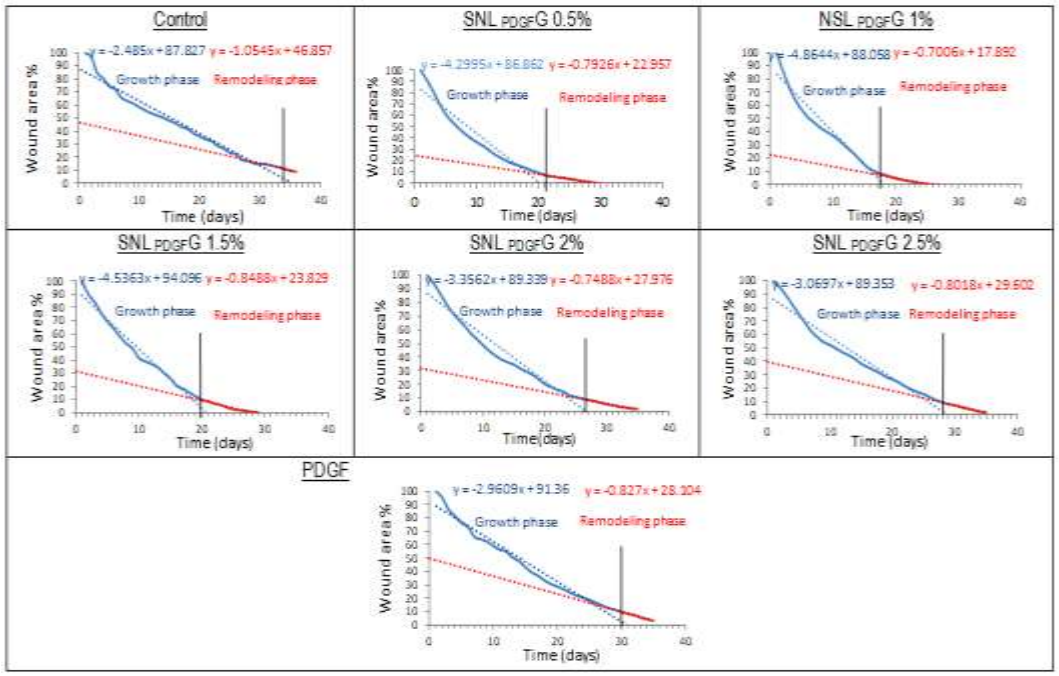

Figure 8. The comparison between wound healing kinetic curves of individual concentration in two-phase growing and remodeling phase in PDGF and Structural Nano-lipid PDGF Gel.

The $SNL_{PDGF}G$, the curve feature of wound healing linear rates and velocities showed the progressive steady increasing value of linear rate with an increased concentration of dressed wounds of $SNL_{PDGF}G$ between control 0 to 1% then tend to disturbance at groups 1.5% - 2.5%, in addition to, the curve of closure $t_{1/2}$ of wound healing were showed advanced decrease value of linear rate with increase in the concentration between 0 to 1% then tend to platen 1% and upset post 1.5% to 2.5%.

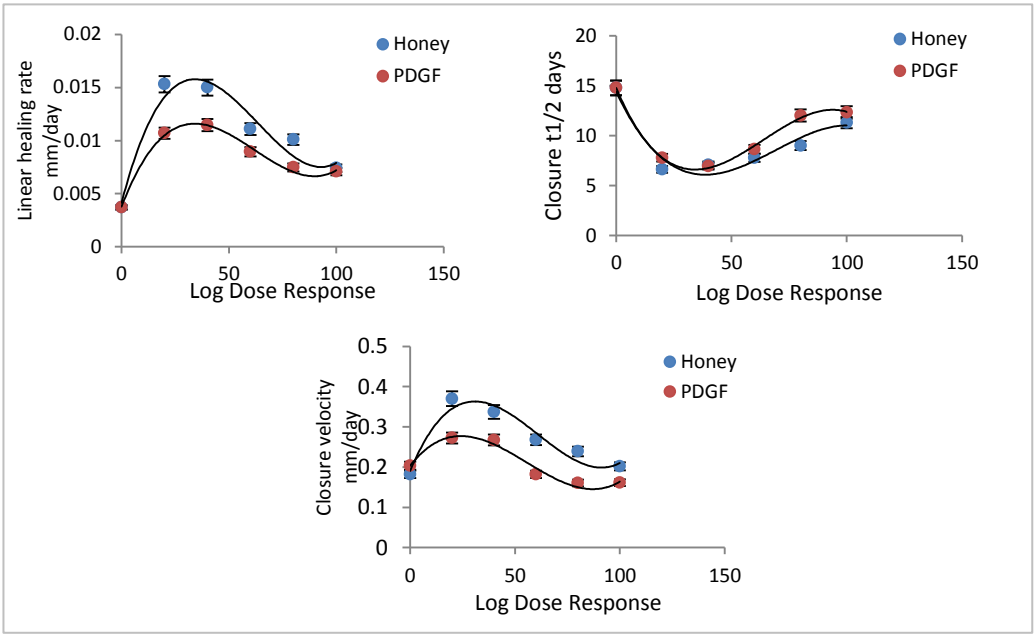

Figure 9. The Log Dose-Response curve of $SNL_{honey}G$ and $SNL_{PDGF}G$ dressed wound versus wound healing indices for linear healing rate, closure $t_{1/2,}$ and closure velocity.

5.5. The effective concentrations ($EC_{s20\ and\ 50}$) of structural Nano-lipid in honey and PDGF

The potencies of dressed different formulas SNL of honey and PDGF were represented in EC_{50} and EC_{20}, the linear healing rate and closure $t_{1/2}$ EC_{50} of honey were lower than closure velocity and there was no difference between linear healing rate and closure $t_{1/2}$, in addition, the closure velocity EC_{20} of $SNL_{honey}G$ lower than linear healing rate and closure time EC_{20}. The linear healing rate and closure $t_{1/2}$ to EC_{50} of PDGF were lower than closure velocity were no significant differences between linear healing rate and closure $t_{1/2}$, while in EC_{20} of PDGF, closure $t_{1/2}$ were lower than linear healing rate and closure velocity were no significant differences between linear healing rate and closure $t_{1/2}$.

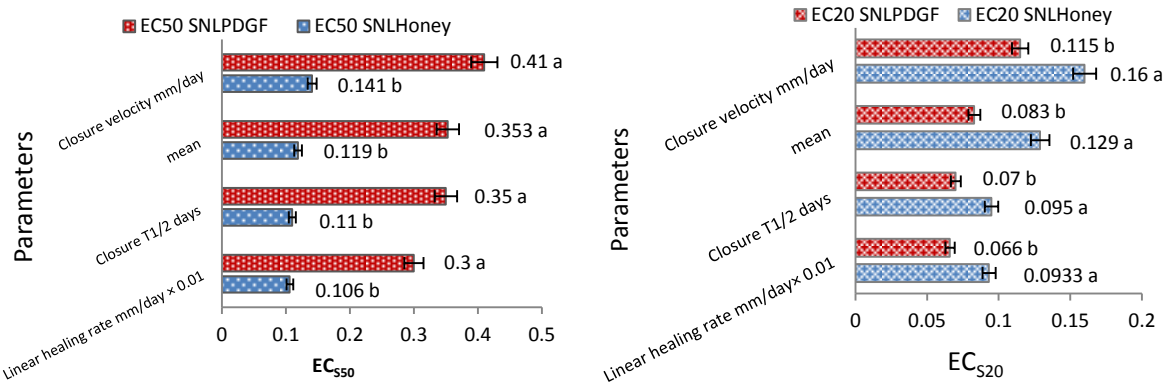

Figure 10. The values of the effective concentration (EC_{S20}) in SNL form in honey and PDGF according to potency

5.6. The isometric score of wound healing in conventional and Structural Nano lipid Honey & PDGF ($SNL_{Honey\ \&\ PDGF}$)

As a measure of comparability and the interplay between traditional and $SNL_{Honey\ \&\ PDGF}$ with uniformity of the growing and remodeling phase, the wound healing process and cellular kinetic competence in regenerated tissue were scored.

Inflammation score: Leucocyte skin infiltration was substantially ($p \leq 0.05$) higher in traditional honey-PDGF, SNL-blank, and control than in $SNL_{Honey\text{-}PDGF}$ during the inflammatory phase of the early formation of the wound. During a longer period of time to heal, the wound groups' leucocyte scores declined negatively, and after 30 days of $SNL_{Honey\ \&\ PDGF}$, the inflammatory cells had completely disappeared.

Scab score: All groups of the wound's scab score declined with time, and on the second day after the wound was first created, scab tissue had begun to form in all groups. The scab score showed the first closure elements inflammatory phase. As opposed to traditional honey-PDGF, which had a higher score, $SNL_{Honey\ \&\ PDGF}$ had a lower score, and the control group's score had declined over the course of healing and after a 20-day absence.

Extracellular matrix deposition: The distribution of fibers in the tissue is a sign of wound closure, and extracellular matrix deposition scores from fibroblast and collagen fiber as the endpoint are taken into account for the second phase of wound healing. $SNL_{Honey\ \&\ PDGF}$ scored higher than control and conventional honey-PDGF, and all groups' extracellular matrix deposition scores increased over the course of the healing process.

Vascularization: The first and second phases of inflammation and fibroblasts were companies with the first and second vascularization score as presented angiogenesis in the wound matrix. The vascularization share dual distribution stages, first, all groups increased scores at the first half of healing periods and significantly decreased the second half. While the maximal vascularization in $SNL_{Honey\ \&\ PDGF}$ at day 7 was lower than remodeling after 28 days, $SNL_{Honey\ \&\ PDGF}$ vascularization scores in the early and second halves of wound healing were higher than conventional and control wounds, respectively.

The Epithelialization Score

All of the epithelialization indicated wound closure and migration of the wound edge to the central wounds. All groups had significantly increased epithelium with increased wound healing time ($p \leq 0.05$), whereas $SNL_{Honey\ \&\ PDGF}$ was significantly higher than conventional $_{Honey\ \&\ PDGF}$, SNL-blank, and control ($p \leq 0.05$), with a significant difference in day 20 between groups.

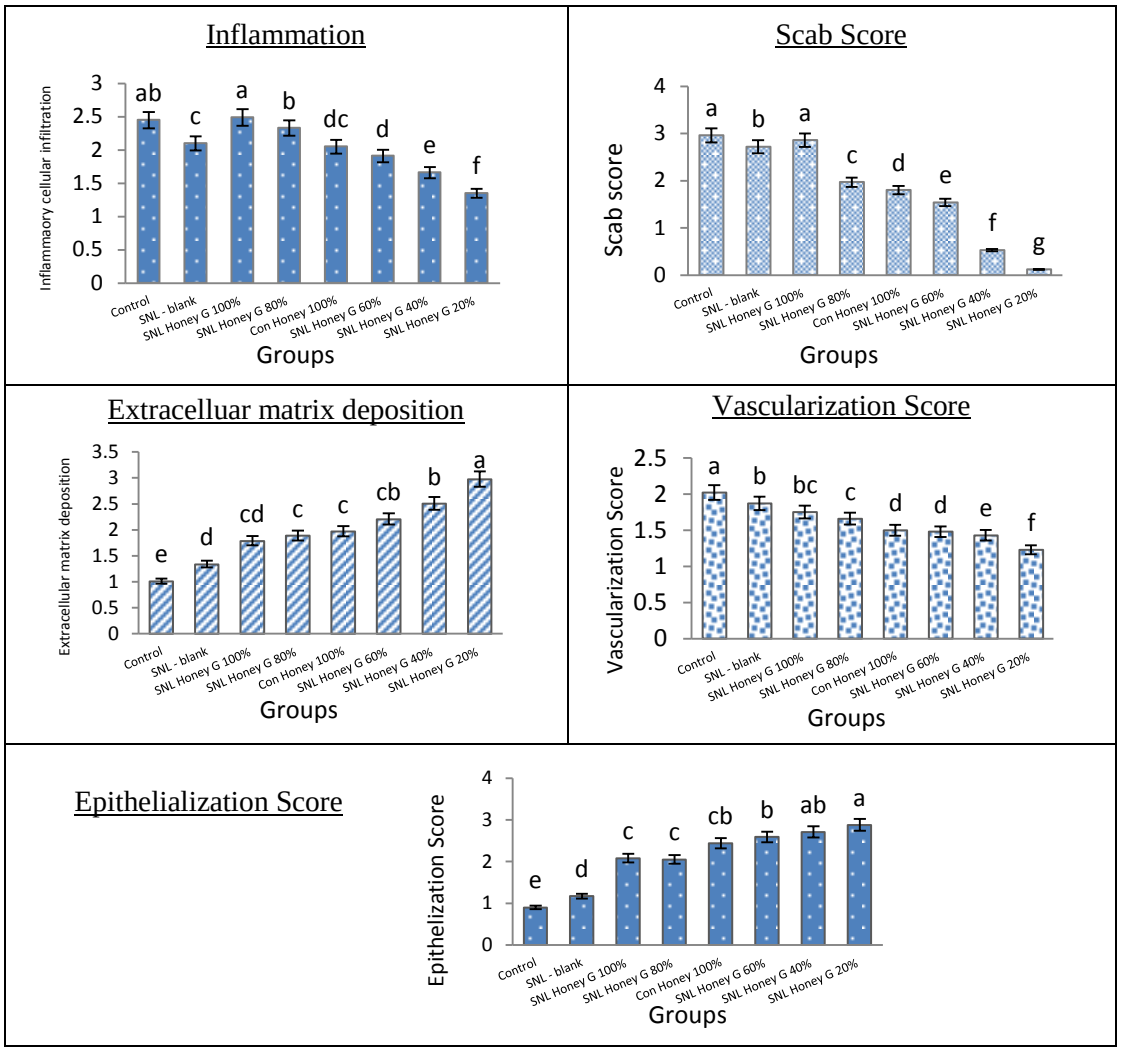

Figure 11. The tissue isometric score of wound healing in honey and Structural Nano-lipid honey (SNL_{Honey}).

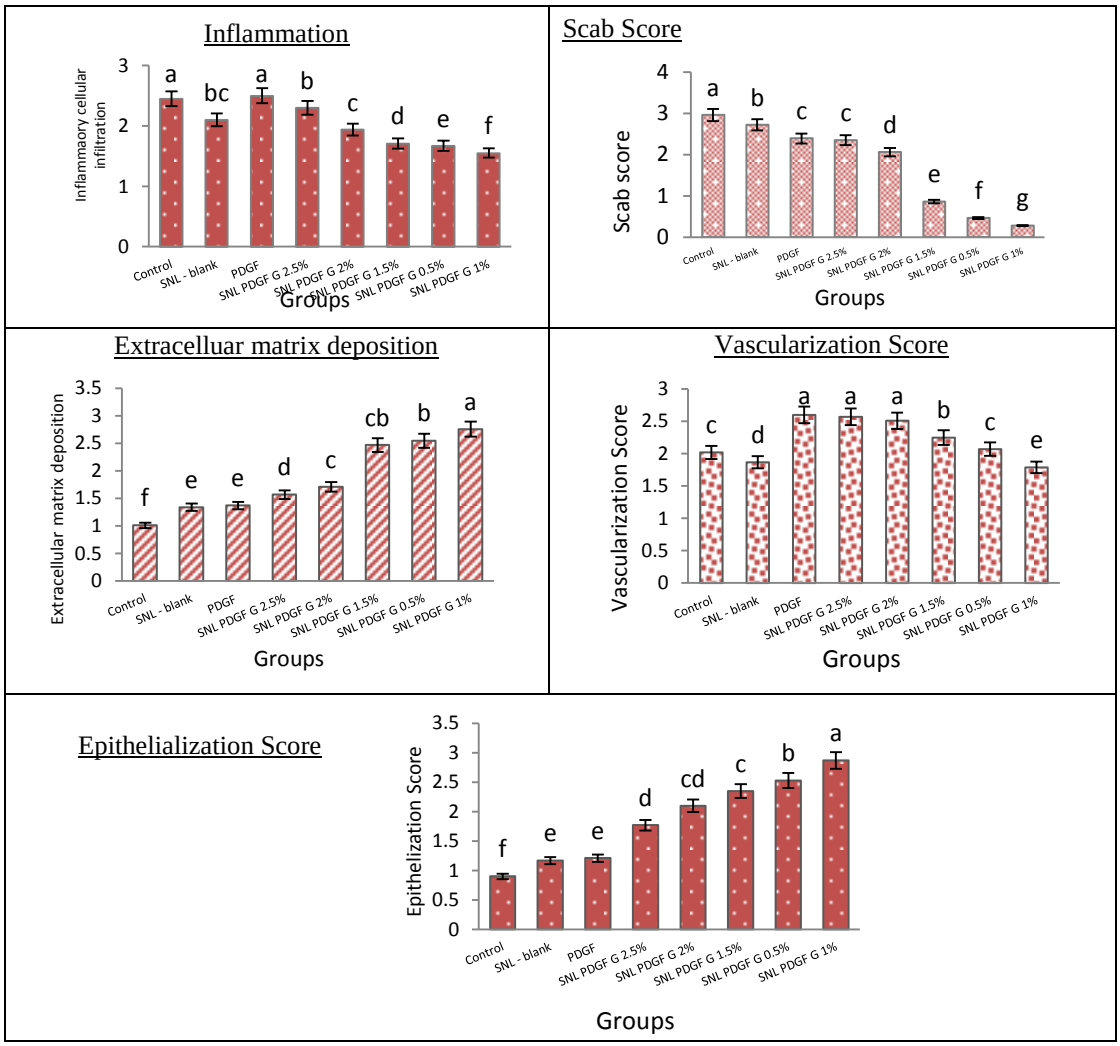

Figure 12. The tissue isometric score of wound healing in PDGF and Structural Nano-lipid PDGF.

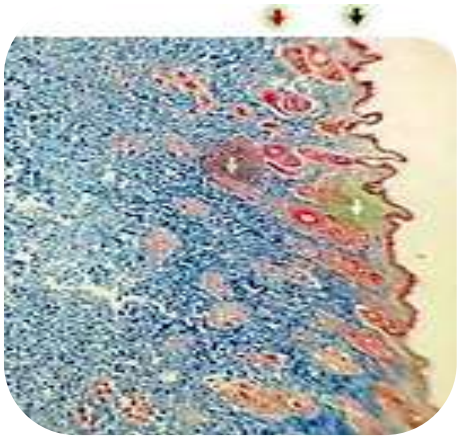

Figure 13. Photomicrographs of normal skin sections stained with Masson trichrome were denoted. The epidermis is shown as a black arrow in the normal histologic appearance of the skin, with a thin keratin layer overlying the epidermis. The connective tissue (collagen and elastic fibers) of dermis layers red arrow, as well as hair follicles green arrow, and sebaceous glands yellow arrow, are found beneath the epidermis.

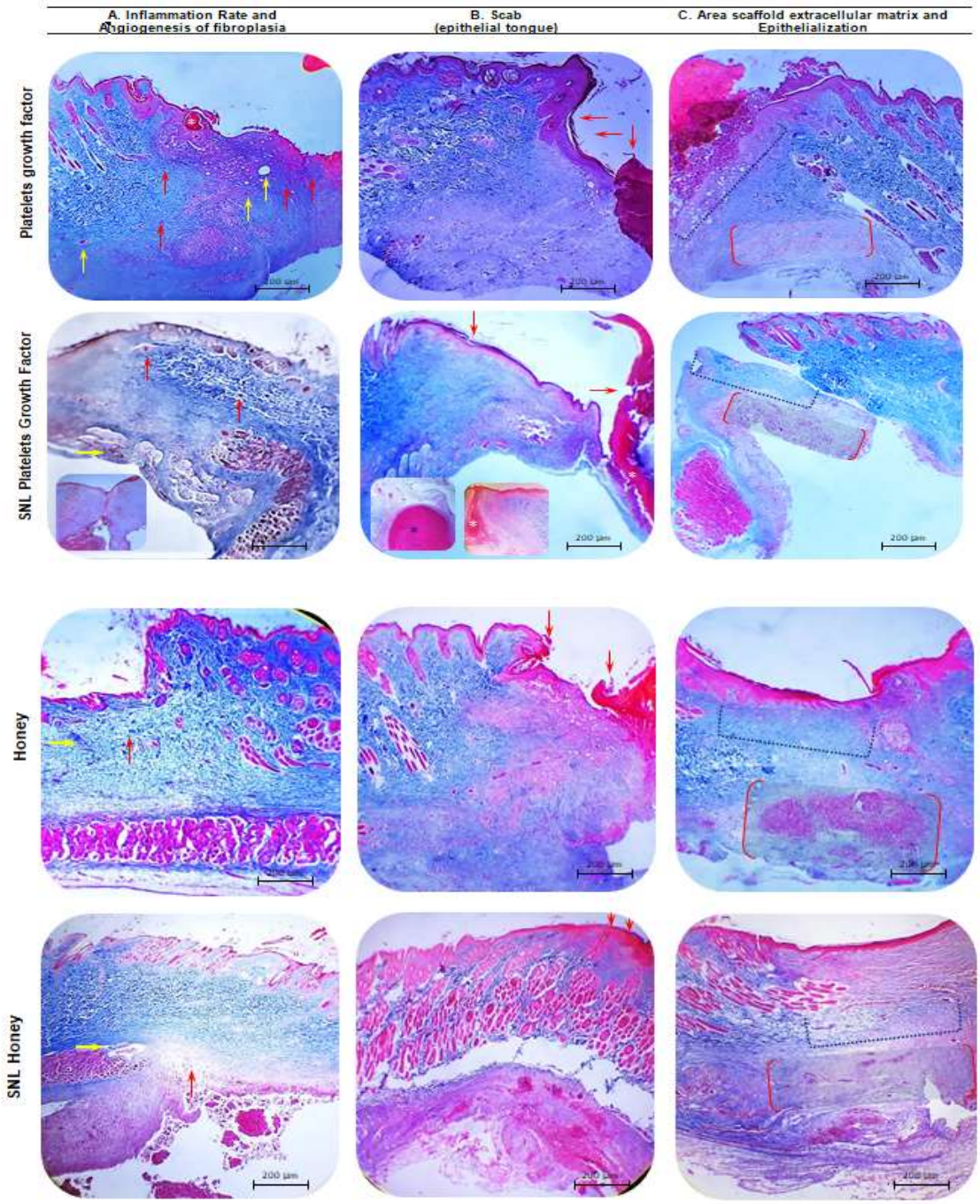

Figure 14. Photomicrographs of skin sections stained with Masson trichrome showing the (A) inflammation rate of cellular infiltration of leukocytes (red arrow) and angiogenesis density of capillary new forming (yellow arrow) in conventional and $SNL_{Honey\ \&\ PDGF}$. In both conventional and $SNL_{Honey\ \&\ PDGF}$, scab epithelial showed a score of scab formation, denoted by the red arrow. (C) In conventional and $SNL_{Honey\ \&\ PDGF}$, the extracellular matrix score was represented by dotted lines, while epithelialization scoring was represented by a red bracket area.

6. Discussion

6.1. Size, Entrapment Efficiency, SEM, and TEM

The size of SNL was determined by lipophilic and covalent forming substances with fatty acid that provide globalization tightly forming with protein containing honey and PDGF and suitable for forming equivalent and forming small size; additionally, the dissolving phase was approved to have miscibility with honey contain that merged with the formation of Nano lipid (Üner, 2016; , Salvi and Pawar, 2019).

Transmission electron microscopy (TEM) and scanning electron microscopy (SEM) were used to determine the size and spherical shape of a Nano lipid. The polymorphic state of lipid due to compatibility with fatty acids and their surfactant, additionally; have both crystallinities throughout the production process and the critical crystallization temperature of this give rigid nanoparticles due to the homogenization step, additionally; the surfactant has a crucial factor that influences the kinetics of lipid Nanoparticle and gives a limited size of globular shape (Tetyczka *et al*., 2019).

Honey-PDGF entrapment is abundant and adequate due to the highly dispersing step of two phases; soluble and particle phases that raged to appropriate surfactant can entrap honey and PDGF, Furthermore, the heterogeneous surfactant and lipid form inner lipid phase with glycerin have drug stability without repulsion out of structure; additionally, the honey of alpha lipoic acid and phenol was shared a good feature and good cationic lipid which presumably increased entrapment and prolong release and entrapment efficiency (Mishra *et al*., 2018).

6.2. Absorbance curve and peaks

The spectral profile was used to quantify the wave length honey of certain amino acid-proteins and phenolic compounds that coincided with their conventional and SNLHoney screen at 271.5, 228.0 that bond amino acid overlapping that may be attributed to SNLHoney not affecting an amino acid honey structure Furthermore, the phenolic compound was found in these bonds overlapping with amino acid. This peak bond may be attributed to polysaccharides and oligosaccharides and maximum absorbance and the same band, which is considered a sole purpose to identify honey and distinguish honey varieties based on the peak functional chemical groups (Brudzynski *et al.*, 2011).

The PDGF absorbance curve displayed a wavelength range between 256.0 and 225.0, which caused the amino acid and the carboxylic groups of saccharides to be exerted in both formulas, resulting in the finding that both concentrations were equal and unified in both, but the absorbance was higher than a conventional due to an excessive increase in the exertion of chemical groups than was embayed in a conventional, as well as the same, is found in the combination of the same wavelength and the amino acid (Kuznetsova *et al.*, 2014).

6.3. X-ray diffraction

The honey amorphous shape was described by Nano form short scattering area, which represents the complete amorphous X-ray diffraction as the same of Gaussian components, which are specified by their amplitude and position (Barud *et al*., 2008).

6.4. Fourier Transform Infrared Spectroscopy

A growth factor, several assessment peaks of the structure-function of honey, SNLhoney, PDGF, and SNLPDGF were examined using Fourier transform infrared spectroscopy (FTIR), and these spectra were correlated with the

corresponding vibrations of function groups. Pure honey's visible region on the FTIR spectrum was 3309.85 cm1, matching SNLhoney's visible region at 3410.15 cm1. this band region is manifested for the stretching vibrations –OH groups found in carbohydrates, water, and organic acids as well as this band was also NH3 stretching band of free amino acids in this region area of scan FTIR (Svecnjak *et al.,* 2015).

The SNLhoney was given a different band due to the exerting of non-binding stretching vibrations that may have a better effect than conventional honey. Conventional honey dealt with exaggerated stretching vibrations of band groups matching with small molecules of growth factor-like behavior compound that were present in honey, which was indicated by the same bond found and matches with PDGF and SNLPDGF (Jedlińska *et al*., 2019).

6.5. Zeta potential of SNL and conventional Honey-PDGF

The particle size distribution with the Nanometric scale was valid in honey -20.1 mV which indicated that $SNL_{Honey,}$ which high values of zeta potential than honey due to its negative charge SNL nature also relatively increase presumably stability suspension and showed repulsion between lipid particles containing honey, which prevent aggregation of Nano lipid particle and this shared stable and dispersed as a fact of mal-tendency to form aggregation (Nair *et al*., 2010).

The SNLPDGF moiety with give the PDGF negative charge without changing their electrical surface stabilizing charge, which can be attributed to the polymeric of SNLPDGF have negative charge play a repulsion activity to less aggregated during synthesis of lipid polymeric loaded matrix. The PDGF have a zeta potential lower than SNLPDGF, which may be due to the effect of acidification bonds, the increasing size of Nano forming lipids, and the moiety of PDGF (Raffin *et al*., 2003).

6.6. Bioassay Challenge of SNL_{Honey} and SNL_{PDG}

Due to its sticky moisture-absorbable complex-containing material in traditional uses of honey that give the same healing fact, which was approved that healing facilitates fact to improved reaction in the wound and interacts with the phasic wound, honey is one of the nutraceuticals used traditionally during ancient times (Sell *et al.,* 2012).

The honey reported by (Yaghoobi *et al*., 2013) was implicated with the reduction of edematous exudate and the edema was reduced due to following the mechanisms, Same evidence was documented in literature was give the honey complete compound antimicrobial effect due to its flavonoid-containing honey which (Abbas *et al*., 2010; Mathew *et al*., 2015) was denoted to circular acid and there ester compound of flavonoid complex, The honey anti-inflammatory play impact all in tissue closure and regeneration of the normal cells this may be due to at hemostasis and blood flow restricted that promote ischemia and oxygen starvation produces hypoxia as well as nutrition lacking (Raynaud *et al*., 2013; Halah and Hussein, 2018).

The honey has another mechanism to accelerate wound healing and evoke the fibroblast during the proliferation phase and growth. The honey-producing hydrogen peroxide and insulin-like growth factor may be stimulated the fibroblast proliferated mechanism and the wound bed angiogenesis. Honey presumably increases collagen forming maybe by increasing the activity of fibroblasts under oxygenated and nutritional demand via massive angiogenesis due

to the acidic media pH via hemoglobin releasing oxygen (Greener *et al.*, 2005).

The low pH promotes epithelialization and may be in dose in wound closure as well as reduce proteases activity which was gave limitation and extracellular matrix removal (ECM) also the low pH of the honey may be acidification that promotes oxygen dissociation from the hemoglobin via Bohr effect and increase oxygenation the cellular demand (Kassim *et al*., 2005).

Generation of Nitric oxide from lymphocyte which was a free radical that act in inflammation and increase wound healing but the overproduction of Nitric oxide at an incorrect time can be led to the progress of pathology related to inflammation there negative correlation between wound healing and inflammation processes (Molan, 2015; Cerovský *et al.*, 2014).

Defensin-1 (Def-1) acted as an antimicrobial peptide source of the bee's hypopharyngeal gland which may prevent bacterial adhesion as modulated extracellular polymeric from bacteria substance production (Bucekova *et al*., 2015: Al-Mohana, 2012). The Defensin-1 derived honey may be a contribution to re-epithelialization with antibacterial properties, then matrix metalloproteinases enzyme 9 (MMP-9) produced by keratinocytes which accelerated keratinocyte migration with facilitated and appear to increase closure rate and decrease $t_{1/2}$ of the closure via increase wound closure velocity (Svensjo *et al*., 2000).

Moisturization of honey texture as presented of free water which accumulates in the wound bed environment providing moisturization and this may presumably act as a preventative of the tissue formation (scar formation) then mitigate dermal necrosis due to air exposure to the wound, In addition, may be attributed honey moisture effect may be facilitating epithelisation and scab reducing as well as granulation tissue faster development (Molan, 2001). So the moisture characteristic of honey accelerated epidermal cell migration opposite to the scab direction. The moisture area due to the honey suggested it is the demand of lymph and water drawing as well as nutrition and oxygenation aids to the injurious tissue (Yao *et al.*, 2016).

The honey has anti-allergic activity this function was reported by that may be reduced eosinophils, interleukin-4, IL-13, and immunoglobulin E (IgE), this fact may be given to minimize etching and etching pain during the healing of dressed wound-mediated histamine release and immunoglobulin as well as cytokines gene expression down-regulation exploration WBC which may be inhibited the caspase-1 relative and NF-κB that presumably reduced hyper responsiveness due to inflammation (Rodrigues *et al*., 2019; Rafiq *et al*., 2022).

The functional and dysfunctional cellular scenario was temporary equilibrium and orchestrate the cells production of inflammatory mediator and growth factors same problems were noted implication in the delay of closure wound and converted the acute wound to the chronic open wound, and the chosen growth factors for improved wound healing indices due to their endogenous factors derived from platelet; (growth factor)(Park *et al.*, 2017). This evidence promotion the media use of growth factors to increase regulate hemostasis and increase the progression of healing and prevent the progression to chronic wounds (Mancuso *et al*., 2017).

The hemostasis of factor regulation healing events and their scenario was initiated by aggregation of platelet-activated factors after exposed the sub-endothelial collagen that forms a plug of the wound and prevents hemorrhage exudation by closed extravasation oozing; which may be promoted primer wound closure (Park *et*

al., 2017). The advanced pathway denoted reduced time closure may be followed the cascade sequence of coagulation and drive the platelet drive growth factors for thrombus formation after inflammatory phases, The PDGF was accelerated proliferative phase to re-epithelialization angiogenesis and collagen deposit with consequences granulation tissue formation (Piipponen *et al*., 2020).

Furthermore, growth factor may be given the responsibility of fibroblast through new generative of extracellular matrix (ECM), the platelet-derived growth factor was inlet facilitated the neo-forming angiogenesis and promotion the dissolving phase as proteolytic enzymes metalloproteinases (MMP) in the basal lamina and surrounding tissue (Hesketh *et al.,* 2017), as well as the platelet-derived growth factor, may be facilitated collagen deposition and scar formation presumably via in increased fibroelastosis-keratinocytosis migration and deposition in early repairing platelet cell activation healing during the inflammatory period (Liu *et al.*, 2021).

The vitality of the growth factor is also the presumable scenario of promoting tissue granulation formation and giving the ability signal transduction regulation between new cells forming then reflected on the regulation of their cell proliferation process migration as well as differentiation of the cells (Park *et al*., 2017).

The raw honey base was previously screened in acute and chronic deep excisional wounds by dressing maneuvers, as well as the fabricated honey for increased efficacy through demand high compatibility, increased area exposure, and highly penetrability, which were allowed bioactive constitutional honey components and PDGF new forming SNL loaded honey-PDGF mimic mutability improved wettability parallel with high bioactivity by SNL and gel the control releasing (65).

The result of wound healing indices showed the superior result that raw or conventional type honey and PDGF that rationally can be attributed to facilitating improved applications of honey-PDGF dressed wound presumably due to high incorporation of drug capacity within Nano, small Nano size within large ratio surface area-volume, as well as improved potency and promising new formula designed for wound healing via achieved bio-pharmaceutics of honey and PDGF delivered system (Khan *et al*., 2019).

The good biocompatibility of SNL-loaded honey and PDGF reported by Zhai and Zhai, (2014) promotes adhesion and penetration to the skin surface and may be due attributed to lipid exchanges and/or looseness of the structure as well as polarity increased hydration effect penetration thus accommodate their penetration and deposition in the deeper layers of cutaneous tissues where the active payload demand the permeability and leakage during their activation of payload the size and structure of Nano lipid was passage as implausible where than passage through the glomerular pathway (Betz *et al*., 2001).

The increased permeability of SNL loaded honey- PDGF molecules in injurious skin damage tissue-specific target layers of the skin, this presumable that the vesicular systems of SNL have amphiphilic molecules at consist hydrophobic and hydrophilic, and play a major fact in increased permeability improved delivered the containing to the deeper skin layer, as well as their small size molecules also potentiate permeability (Duan *et al*., 2020).

This skin penetration efficiency was reported by Sala *et al.* (2018) attributed to increased solubility and diffusion ability through the skin, which enhanced physical and mechanical passing velocity on targeted delivery into specific layers of growing associated with decreased dosage amount with the side effect.

Furthermore, the goal of SNL delivery formulation of honey-PDGF was presumably increased preventative before infection with enhancing re-epithelization short term for increased skin integrity and function and previously mention, exhibited antibacterial effect and re-epithelization promoter associated with the overcome phenomenon of resistance rate antibiotics (Ali et al., 2018) also Han and Ceilley, (2017) suggest the SNL maybe prevent promoted of inflammatory phase with the promotion of angiogenesis and scavenging of reactive oxygen radical for avert of conversion acute wound to the chronic wound, all of these may be terminated on the SNL play raw of increase of honey-PDGF $t_{1/2}$ and skin bio viability and associated minimize toxicity.

The result of SNL honey-PDGF treated groups were improved as compared with conventional honey-PDGF may be attributed to the SNL formula suggested was approved efficiency via high stability, high capacitation of drug, and slow sustained release of drugs, and improved drugs function by exhibiting low allergenic and toxic profile eg; at first low concentration in experimental that reduced dressing and application number and reduced healing time, which agree with our results of timeline scars of SNL honey-PDGF (Chato-Astrain *et al.*, 2020).

The SNL basic matric of Nano forming formula may be increased skin collagen excessive amount in the remodelling phase, which was agreed with groups SNL-blank treated groups that showed histologically and grossly forming hypertrophic scars and keloid forming. Furthermore, another attribution the transition time of SNL loaded drug was generally prolonged that facilitated to transduction of the corneum stratum penetrating to avascular corneous this is presumably attributed to fluidization delivery of active honey-PDGF beneath the layer of cutaneous layers and diffusible horizontally via trans cellular and intercellular transition of drugs (Grubbs and Manna, 2020; Hua, 2015).

This fact agreed with the study result of the histological appearance of wound healing as well as reflected on potencies percent displayed honey more potencies than growth factor, in addition, the linear timeline of wound kinetic healing showed the groups of honey had a shorter time of healing than PDGF in conventional treatment permission shad the light on uses of reformulated PDGF in biotechnological pharmaceutics that run PDGF loaded with SNL and for protect and control release PDGF may be the certain result was achieved and as well as protected PDGF during the processing of cold SNL process and at time distractive SNL PDGF during exposure at dress wound. These give advantages may be prolonged release and control amount liberation that may prevent the conversion of acute to chronic form as well as was held on gel at SNL form of PDGF which both of them SNL and gel act as delivery system topically (Losi *et al.*, 2013; Boateng and Catanzano, 2015).

7. Conclusions

The reformulated conventional $_{\text{Honey\& PDGF}}$ acquired the status of Nanoparticles through carrying it in structure Nano lipid that $SLN_{\text{Honey\& PDGF}}$ has different advantages in delivery systems for topical application and accelerated wound healing. The $SLN_{\text{Honey\& PDGF}}$ efficiency was preferred to conventional $_{\text{Honey\& PDGF}}$ having a good onset of action in skin wound healing. The dressed of the excisional wound of skin in $SLN_{\text{Honey\& PDGF}}$ gel work on accelerated wound healing and overcomes the side effect of delaying healing indicated by increased linear healing rate and closure velocity and decreased half-life.

8. Recommendations

An Extension of the idea of developing and surveying activities of Honey and PDGF in Nano form on the body is assumed as follows:

1. Clinical usage of a new formulation of $SNL_{Honey\&\ PDGF}$ in the wound of large animals.
2. Further comparative *in vitro* and *in vivo* studies are required to elucidate $SNL_{Honey\&\ PDGF}$ used in burn wounds.

REFERENCES

Ramli, NZ., Chin, KY., Zarkasi, KA. And Ahmad, FA. 2018. Review on the Protective Effects of Honey against Metabolic Syndrome. Nutrients., 10(8): 1009.

Burlando, B. and Cornara, L. 2013. Honey in dermatology and skin care: a review. J Cosmet Dermatol., 12(4): 306-313.

Duncan, HF., Kobayashi, Y. and Shimizu, E. 2018. Growth factors and cell homing in dental tissue regeneration. Curr Oral Health Rep., 5(1): 276–85.

Evans, BC., Fletcher, RB. and Kilchrist, KV. 2019. An anionic, endosome-escaping polymer to potentiate intracellular delivery of cationic peptides, biomacromolecules, and nanoparticles. Nat Commun., 10(2): 1–19.,

Silva, MMP., Aguiar, MIF., Rodrigues, AB., Miranda, MDC., Araújo, MÂM. and Rolim, ILTP. 2018. "The use of nanoparticles in wound treatment: a systematic review". Rev Esc Enferm USP, 8(51): e03272.

Campos, J.R., Severino, P., Santini, A., Silva, A.M., Shegokar, R., Souto, S.B. and Souto, E.B. 2020. Chapter 1-Solid lipid nanoparticles (SLN): Prediction of toxicity, metabolism, fate and physicochemical properties. In Nanopharmaceuticals; Shegokar, R., Ed.; Elsevier: Amsterdam, The Netherlands, pp. 1–15.

Zhang, J., Xiao, X. and Zhu, J. 2018. Lactoferrin-and RGD-comodified, temozolomide and vincristine-coloaded nanostructured lipid carriers for gliomatosis cerebri combination therapy. Int J Nanomedicine. 13(1): 3039-3051.

Buthina, A Abdullaha, Mohanad, A AL-Bayati. 2023. Production and Characterization of Nanostructured-Lipid Carriers as Hormones PGF2αand PMSG. The Egyptian Journal of Hospital Medicine, 90(1): 412-420.

Cohen, R., Kanaan, H., Grant, J.C. and Barenhol, Z.Y. 2012. Prolong analgesia from Bupisone & Bupigel formulations: from design & fabrication to improved stability. Journal of Control Release, 160(2): 346-352.

Sivakumaran, D., Maitland, D. and Hoare, T. 2011. Injectable Microgel- Hydrogel Composites for Prolonged Small – Molecule Drug Delivery. Journal of Biomacromolecules, 12(11): 4112-20.

Nawal, S. Jaafer, Balqees, H.A. and Mohanad, A. Al-Bayati. 2020. Preparation and Standardization of Liposomes Encapsulated Newcastle Disease Vaccine in Unilamellar and multilamellar forms. Plant Archives., 20(1): 978-982.

Mathur, V., Satrawala, Y. and Rajput, M.S. (2014). Physical and chemical penetration enhancers in transdermal drug delivery

system. Asian Journal, of Pharmaceutics (AJP), 4(3): 143.

Yokoyama, T., Fukui, T. and Masuda, H. 2007. Chapter 1: Basic Properties and Measuring Methods of Nanoparticles. Journal of Nanoparticle Technology Handbook (edited by: Hosokawa, M.; Nogi, K.; Naito, M.;Yokoyama, T.).

Zine, R. and Sinha, M. 2017. Nanofibrous poly(3-hydroxybutyrate-co3-hydroxyvalerate)/collagen/graphene oxide scaffolds for wound coverage. Materials Science and Engineering Journal, 1(80): 129-134.

Wang, T., Lin, J., Chen, Z., Megharaj, M. and Naidu, R. 2014. Green synthesized iron nanoparticles by green tea and eucalyptus leaves extracts used for removal of nitrate in aqueous solution. Journal of Cleaner Production, 83(2): 413-419.

Wang, J., Zhang, L., Chi, H. and Wang, S. 2016. An alternative choice of lidocaineloaded liposomes: lidocaine-loaded lipid-polymer hybrid nanoparticles for local anesthetic therapy. Drug Deliv., 23(4): 1254-1260.

Ali, M. Ghazi and Mohanad, A Al-Bayati. 2020. Anti-proliferative of the phytosome propolis, phytosome lycopene and synergistic effect on the benign prostatic hyperplasia cells in-vitro. Plant Arch., 20(1): 6579-6589.

Balbino, C.A., Pereira, L.M. and Curi, R. 2005. Mechanisms involved in wound healing: arevision. Rev Bras Cienc Farm., 41(1): 27-51.

Roaa, K J. and Mohanad, A. Al-Bayati. 2022. Preparation and standardizations of structural nano- lipid loaded lidocaine and conventional lidocaine. International Journal of Health Sciences., 6(S1): 14145-14156.

Camila, D., Carolina, C. and Marcelo, S. 2015. Time-resolved and steady-state fluorescence spectroscopy for the assessment of skin photoaging process. Journal of SPIE digital library., 5(1): 44-48.

Canesso, M. C., Vieira, A. T., Castro, T. B., Schirmer, B. G., Cisalpino, D., Martins, F.S., Rachid, M. A., Nicoli, J. R., Teixeira, M. M. and Barcelos, L. S. 2014. Skin wound healing is accelerated and scarless in the absence of commensal microbiota. Journal of Immunology, 193(10): 5171-80.

Vidal, X., Cheung, S. and Chiapolini, N. 2015. Observation of J/ψp Resonances Consistent with Pentaquark States in Λ0b→J/ψK−p Decays. Journal of Physical Review Letters., 33(14): 32-36.

Gopinath, D., Ahmed, M. R., Gomathi, K., Chitra, K., Sehgal, P.K. and Jayakumar, R. 2004. Dermal wound healing processes with curcumin incorporated collagen films. Journal of Biomaterials, 25(10): 1911-1917.

Roaa, K J. and Mohanad, A. Al-Bayati. 2022. preparation and standardization of structural Nano-lipid loaded lidocaine and conventional lidocaine. International Journal of Health Sciences., 2(3):18-21.

Cassini-Vieira, P., Moreira, C. F., da Silva, M. F. and Barcelos, L. S. 2015. Estimation of wound tissue neutrophil and macrophage accumulation by measuring myeloperoxidase (MPO) and N-Acetylβ-D-glucosaminidase (NAG) activities. Journal of Bio-protocol, 5(22): e1662.

Gilman T. 2004. Wound Outcomes: The Utility of Surface Measures. The International Journal of Lower Extremity Wound, 3(3): 125-132.

Vidal, X., Cheung, S. and Chiapolini, N. 2015. Observation of J/ψp Resonances Consistent with Pentaquark States in Λ0b→J/ψK−p

Decays. Journal of Physical Review Letters., 33(14): 32-36.

Muhannad, A. Al Bayaty. 2005. Quantitation of Leydig cell in testicular biopsies of gossypol treated rats. The Iraqi Journal of Veterinary Medicine., 29(1): 179-189.

Cassini-Vieira, P., Moreira, C. F., da Silva, M. F. and Barcelos, L. S. 2015. Estimation of wound tissue neutrophil and macrophage accumulation by measuring myeloperoxidase (MPO) and N-Acetylβ-D-glucosaminidase (NAG) activities. Journal of Bio-protocol, 5(22): e1662.

Castro, B., Maria, C. and Angélica, T. (2014). Skin wound healing is accelerated and scarless in the absence of commensal microbiota. Journal of Immunology. 193(10): 5171-80.

de Moura Estevão, LR., Cassini-Vieira, P., Leite, AGB., de Carvalho Bulhões, AAV., da Silva Barcelos, L. and Evêncio-Neto, J. 2019. Morphological Evaluation of Wound Healing Events in the Excisional Wound Healing Model in Rats. Journal of Bioprotocol, 9(13): e3285.

Fatima, M. and Al-Bayati, M. 2021. The Reproductive Effect of Liposomal Cimetidine on Adult Male Mice. Plant Archives Journal., 21 (1): 757-769.

Al-Bayati, M.A. and Khames, W. 2015. Importance of following standardized guideline for the care and use for laboratory animals in research and teaching in Iraqi scientific institutions FIQ. J. Med. Sci., 2: 11-14.

Tome O. H. 2009. Comparaision of calibration curve fitting methods in absorption spectroscopy, Anal. Chem., 1976(48): 312-318.

Üner, M. 2016. Characterization and Imaging of Solid Lipid Nanoparticles and Nanostructured Lipid Carriers. In Handbook of Nanoparticles; Aliofkhazraei, M., Ed.; Springer International Publishing: Cham, Switzerland, pp. 117-141.

Salvi, V.R. and Pawar, P. 2019. Nanostructured Lipid Carriers (NLC) System: A Novel Drug Targeting Carrier. J. Drug Deliv. Sci. Technol., 51(1): 255-267.

Tetyczka, C., Hodzic, A., Kriechbaum, M., Jurai´c, K., Spirk, C., Hartl, S., Pritz, E., Leitinger, G. and Roblegg, E. 2019. Comprehensive Characterization of Nanostructured Lipid Carriers Using Laboratory and Synchrotron X-Ray Scattering and Diffraction. Eur. J. Pharm. Biopharm., 139(3): 153-160.

Mishra, V., Bansal, K., Verma, A., Yadav, N., Thakur, S., Sudhakar, K. and Rosenholm, J. 2018. Solid Lipid Nanoparticles: Emerging Colloidal Nano Drug Delivery Systems. Pharmaceutics, 10(4): 191.

Brudzynski, K., Abubaker, K., St-Martin, L. and Castle, A. 2011. Re-examining the role of hydrogen peroxide in bacteriostatic and bactericidal activities of honey. Front. Microbiol, 2(1): 213.

Kuznetsova, I.M., Turoverov, K.K. and Uversky, V.N. 2014. What macromolecular crowding can do to a protein? Int. J. Mol. Sci., 15(12): 23090–23140.

Barud, HS., Araújo-Júnior, AM., Santos, SB., Assunção, RM., Meireles, CS., Cerqueira, DA., Rodrigues-Filho, G., Ribeiro, CA., Messaddeq, Y. and Ribeiro, SJ. 2008. Thermal behavior of cellulose acetate produced from homogeneous acetylation of bacterial cellulose. Thermochimica Acta., 471(1-2): 61-69.

Svecnjak, L., Bubalo, D., Baranovic, G. and Novosel, H. 2015. Optimization of FTIR-ATR spectroscopy for botanical authentication of unifloral honey types and

melissopalynological data prediction. Eur. Food Res. Technol., 240(6): 1101-1115.

Jedlińska A. 2019. The application of dehumidified air in rapeseed and honeydew honey spray drying—process performance and powders properties considerations. J. Food Eng. 245(1): 80–87.

Nair, HB., Sung, B., Yadav, VR., Kannappan, R., Chaturvedi, MM. and Aggarwal, BB. 2010. Delivery of antiinflammatory nutraceuticals by nanoparticles for the prevention and treatment of cancer. Biochem Pharmacol., 80(12): 1833-1843.

Raffin, RP., Obach, ES., Mezzalira, G., Pohlmann, AR. and Guterres, SS. 2003. Nanocápsulas poliméricas secas contendo indometacina: estudo de formulação e tolerância gastrintestinal em ratos. Acta Farmacêutica Bonaerense, 22(2): 163-172.

Sell, SA., Wolfe, PS. and Spenec, AJ. 2012. A preliminary study on the potential of manuka honey and platelet-rich plasma in wound healing. Int J Biomater., 2012(3): 313781.

Yaghoobi, R., Kazerouni, A. and Kazerouni, O. 2013. Evidence for clinical use of honey in wound healing as an anti-bacterial, anti-inflammatory anti-oxidant and anti-viral agent: a review. Jundishapur J Nat Pharm Prod., 8(3): 100-104.

Mathew, S., Abraham, T.E., Zakaria, Z.A. 2015. Reactivity of phenolic compounds towards free radicals under in vitro conditions. J. Food Sci. Technol., 52(9): 5790-5798.

Raynaud, A., Ghezali, L., Gloaguen, V., Liagre, B., Quero, F. and Petit, JM. 2013. Honey-induced macrophage stimulation: AP-1 and NF-kB activation and cytokine production are unrelated to LPS content of honey. Int Immunopharmacol., 17(3): 874-879.

Greener, B., Hughes, A.A., Bannister, N.P. and Douglass, J. 2005. Proteases and pH in chronic wounds. J. Wound Care, 14(2): 59-61.

Kassim, M., Achoui, M., Mansor, M. and Mohd, K. 2010. The Inhibitory Effects of Gelam Honey and Its Extracts on Nitric Oxide and Prostaglandin E 2 in in Fl Ammatory Tissues. Fitoterapia, 81(8): 1196-1201.

Molan, P. and Rhodes, T. 2015. Honey: A Biologic Wound Dressing. Wounds, 27(6): 141-151.

Cerovský, V., Bém, R. and Lucifensins, A. 2014. the Insect Defensins of Biomedical Importance: The Story behind Maggot Therapy. Pharmaceuticals., 7(2): 251–264.

Bucekova, M., Buriova, M., Pekarik, L., Majtan, V. and Majtan, J. 2018. Phytochemicals-mediated production of hydrogen peroxide is crucial for high antibacterial activity of honeydew honey. Sci. Rep., 8(1): 9061.

Svensjo, T., Pomahac, B., Yao, F., Slama, J. and Eriksson, E. 2000. Accelerated healing of full-thickness skin wounds in a wet environment. Plast. Reconstr. Surg., 106(3): 602-612.

Molan, PC. 2001. Honey as a topical antibacterial agent for treatment of infected wounds. World Wide Wounds, 6(3): 1-13.

Yao, J., Jiang, M., Zhang, Y., Liu, X., Du, Q. and Feng, G. 2016. Chrysin alleviates allergic inflammation and airway remodeling in a murine model of chronic asthma. Int Immunopharmacol., 32(2): 24-31.

Rodrigues, M., Kosaric, N., Bonham, C. A., and Gurtner, G. C. 2019. Wound healing: A cellular perspective. Physiol. Rev., 99(1): 665-706.

Broszczak, DA., Sydes, ER., Wallace, D. and Parker, TJ. 2017. Molecular Aspects of Wound Healing and the Rise of Venous Leg Ulceration: Omics Approaches to Enhance Knowledge and Aid Diagnostic

Discovery. Clin Biochem Rev., 38(1): 35-55.

Mancuso, M.E. and Santagostino, E. 2017. Platelets: Much More than Bricks in a Breached Wall. Br. J. Haematol., 178(2): 209-219.

Piipponen, M., Li, D. and Landén, N.X. 2020. The Immune Functions of Keratinocytes in Skin Wound Healing. Int. J. Mol. Sci., 21(22): 8790.

Hesketh, M., Sahin, K.B., West, Z.E. and Murray, R.Z. 2017. Macrophage Phenotypes Regulate Scar Formation and Chronic Wound Healing. Int. J. Mol. Sci., 18(7): 1545.

Liu, Y., Li, T., Han, Y., Li, F. and Liu, Y. 2021. Recent development of electrospun wound dressing. Curr. Opin. Biomed. Eng., 17(1): 100247.

Khan, I., Saeed, K. and Khan, I. 2019. Nanoparticles: Properties, Applications and Toxicities. Arab. J. Chem., 12(7): 908-931.

Zhai, Y. and Zhai, G. 2014. Advances in lipid-based colloid systems as drug carrier for topic delivery. J. Control. Release, 193(168): 90-99.

Betz, G., Imboden, R. and Imanidis, G., 2001. Interaction of liposome formulations with human skin in vitro. Int. J. Pharm., 229(1-2): 117-129.

Duan, Y., Dhar, A., Patel, C., Khimani, M., Neogi, S., Sharma, P., Siva Kumar, N. and Vekariya, R.L. 2020. A Brief Review on Solid Lipid Nanoparticles: Part and Parcel of Contemporary Drug Delivery Systems. RSC Adv., 10(45): 26777-26791.

Determination of Water-Soluble Vitamins in Iraqi Honey Bee and Compare with Others Types by High –Performance Liquid Chromatography

Rafiq, M.S. Rashid, Reder R. Mohammed, salih and Dalia A. Ali. 2022. Glycemic response of honey and dates consumption, Baghdad Journal of Biochemistry and Applied Biological Sciences, 3(01): 17-28.

Sala, M., Diab, R., Elaissari, A. and Fessi, H. 2018. Lipid nanocarriers as skin drug delivery systems: Properties, mechanisms of skin interactions and medical applications. International Journal of Pharmaceutics, 535(2): 1-17.

Ali, M., Jahromi, M., Zangabad, P.S., Moosavi, S.M., Zangabad, K.S., Ghamarypour, A., Aref, A.R., Hamblin, M.R. and Education, U.S. 2018. Education, U.S. Nanomedicine and Advanced Technologies for Burns: Preventing Infection and FacilitatingWound Healing. Adv. Drug Deliv. Rev., 123(1): 33-64.

Al-Mohana, A.M.G. 2012. Biological activity of local honey bees in growth of some gram positive and negative bacteria, The Iraqi Journal of Veterinary Medicine, 36(1): 15-24.

Han, G. and Ceilley, R. 2017. ChronicWound Healing: A Review of Current Management and Treatments. Adv. Ther., 34(3): 599-610.

Chato-Astrain, J., Chato-Astrain, I., Sánchez-Porras, D., García-García, Ó.D., Bermejo-Casares, F., Vairo, C., Villar-Vidal, M., Gainza, G., Villullas, S. and Oruezabal, R.I. 2020. Generation of a Novel Human Dermal Substitute Functionalized with AntibioticLoaded Nanostructured Lipid Carriers (NLCs) with Antimicrobial Properties for Tissue Engineering. J. Nanobiotechnol., 18(174): 1-13.

Grubbs, H. and Manna, B. 2020. Wound Physiology. In StatPearls; StatPearls Publishing: Treasure Island, FL, USA.

Hua, S. 2015. Lipid-Based Nano-Delivery Systems for Skin Delivery of Drugs and

Bioactives. Front. Pharmacol., 6(219): 2011-2015.

Losi, P., Briganti, E. and Errico, C. 2013. Fibrin-based scaffold incorporating VEGF- and bFGF-loaded nanoparticles stimulates wound healing in diabetic mice. Acta Biomater., 9(8): 7814-7821.

Boateng, J. and Catanzano, O. 2015. Advanced therapeutic dressings for effective wound healing-a review. J Pharm Sci., 104(11): 3653-3680.

Abbas, H.N. Al-saeed, Saffaa, A.A. and Ali, A. Abed Al-abbas. 2010. Inhibitory effect of local Honey on Bacteria in culture media and in laboratory animals. The Iraqi Journal of Veterinary Medicine, 34(1): 103-110.

Halah, M. and Hussein, AL-Hasani. 2018. Study Antibacterial Activity of Honey Against Some Common Species of Pathogenic Bacteria.Iraqi Journal of Science, 59(1A): 30-37.